Effect of Annealing on the Main-Chain Motions of Poly(butylene terephthalate)

Joel R. Garbow† and Jacob Schaefer*‡

Physical Sciences Center, Monsanto Company, St. Louis, Missouri 63167.
Received September 26, 1986

ABSTRACT: Spin–lattice T_1(C) and $T_{1\rho}$(C) relaxation and C–H dipolar line shapes have been obtained for the ring and aliphatic carbons of quenched and annealed poly(butylene terephthalate) by ^{13}C NMR. At room temperature the rings in a fraction of the amorphous regions undergo large-amplitude motions consistent with 180° flips superimposed on wiggles and oscillations. Amplitudes of the motions of the two types of methylene carbon of the butylene moiety are smaller and differ in the annealed but not in the quenched material. This contrast suggests the importance of interchain packing in determining cooperative main-chain motions in the amorphous regions of the polymer.

Introduction

Jelinski and co-workers have shown convincingly that the rings in the amorphous regions of poly(butylene terephthalate) (PBT) undergo rapid 180° flips superimposed on oscillations about the ring C_2 axis[1] and that the butylene carbons undergo motions of the defect-diffusion type[2] suggested by Helfand.[3,4] These determinations were made by ^{2}D NMR on three specifically deuteriated samples at temperatures above the T_g of the amorphous component.

We have been using two-dimensional dipolar rotational spin-echo (DRSE) ^{13}C NMR[5-7] in an effort to understand the physics controlling motions like ring flips in glassy polymers[8] at their normal use temperatures of $T < T_g$. The DRSE experiment is well suited to this application. The experiment is performed on natural-abundance materials and yields a dipolar line shape for each carbon resonance resolved by decoupling and magic-angle spinning. Minor differences between motions of similar carbons in the repeat unit are therefore not obscured by the sample-to-sample variations possible with preparations of specifically labeled materials. Since the ^{13}C–^{1}H dipolar interaction is only about 20 kHz, data collected in the DRSE spectral window require no special precautions or subsequent corrections. In this paper we report the results of DRSE ^{13}C NMR experiments performed on partially crystalline PBT which suggest that the motions of both ring and aliphatic carbons are strongly influenced by interchain packing in the amorphous regions of the solid.

Experiments

Magic-Angle Spinning and Relaxation Measurements. Cross-polarization magic-angle spinning ^{13}C NMR spectra and relaxation measurements were obtained at room temperature on a spectrometer built around a 12-in. iron magnet operating at a proton Larmor frequency of 60 MHz.[9] Half-gram samples were spun in a double-bearing rotor[10] at 1859 Hz. T_1(C) was measured by the Torchia method[11] and $T_{1\rho}$(C) by standard procedures.[12]

Carbon Dipolar Sideband Patterns. Carbon dipolar line shapes were characterized by DRSE ^{13}C NMR at 15.1 MHz. This is a two-dimensional experiment[13] in which, during the additional time dimension, carbon magnetization is allowed to evolve under the influence of C–H coupling while H–H coupling is suppressed by homonuclear multiple-pulse semiwindowless MREV-8 decoupling.[14] The cycle time for the homonuclear decoupling pulse sequence was 33.6 μs, resulting in decoupling of proton–proton interactions as large as 60 kHz (1/16.8 μs). Sixteen MREV-8 cycles fit exactly into one rotor period so that strong dipolar echoes formed. For singly protonated carbons whose resonances are well resolved in the chemical-shift dimension, a Fourier transform of the intensity at the echo maximum vs. evolution time yields a dipolar spectrum consisting of a ^{13}C–^{1}H Pake doublet, scaled by the MREV-8 decoupling, and broken up into sidebands by the magic-angle spinning.[5] The dipolar pattern for a methylene carbon is more complicated and can be thought of as the superposition of two patterns, one with proton spins parallel and the other with proton spins antiparallel. Molecular motion modifies all these patterns just as it does quadrupolar line shapes.[15]

Table I
^{13}C Spin-Lock Lifetimes for Poly(butylene terephthalate)

thermal history	H_1(C), kHz	⟨$T_{1\rho}$(C)⟩,[a] ms: protonated aromatics[b]	⟨$T_{1\rho}$(C)⟩,[a] ms: –OCH_2–	⟨$T_{1\rho}$(C)⟩,[a] ms: –CH_2–
quenched	60	13.5	10.3	8.0
	50	13.4	9.7	7.3
	44	13.0	9.0	7.2
	37	11.1	6.0	5.2
annealed	60	23.7	9.3	7.2
	50	22.9	7.8	6.4
	44	22.0	7.8	6.4
	37	16.9	6.1	5.4

[a] Least-squares fit (97% confidence level) to the observed decay between 0.05 and 1.00 ms after the turnoff of H_1(C). [b] Resonance at 128 ppm. Overlap with 132 ppm peak not removed by computer deconvolution.

Materials. Dried PBT (Polysciences, Inc.) was heated to 250 °C for 3 min, pressed into thin disks, and then quenched in ice water from the melt. Annealing was done at 110 °C (above the T_g of 50 °C but below the T_c of 223 °C) for 260 h under an atmosphere of N_2. The annealing temperature was lowered to room temperature over a 2-h period. The thin-disk geometry ensured that the PBT samples were not subsequently stressed by the magic-angle spinning.

Results

Line Assignments and Relaxation Rates. The ^{13}C NMR spectrum of quenched PBT, $-(C_6H_4C(=O)-OCH_2CH_2CH_2CH_2OC(=O))-_x$, is shown in Figure 1 (top left). The five-line spectrum is assigned[16] to carbonyl carbons (165 ppm), nonprotonated aromatic carbons (132 ppm), protonated aromatic carbons (128 ppm), –OCH_2– methylene carbons (63 ppm), and interior –CH_2– methylene carbons (23 ppm). Because of a short proton $T_{1\rho}$ in PBT, a 2-ms proton–carbon cross-polarization contact enhances the nonprotonated carbon intensities more than the protonated-carbon intensities.[9] Spinning sidebands are minor and do not overlap isotropic peaks. The aromatic region can be resolved by computer simulation using two Lorentzians with minor Gaussian character (Figure 1, right). The intensities of the dipolar echoes following 16 MREV-8 cycles are about 70% for the singly protonated carbons and 60% for the doubly protonated carbons

† Present address: Life Sciences NMR Center, Monsanto Co., Chesterfield, MO 63198.
‡ Present address: Department of Chemistry, Washington University, St. Louis, MO 63130.

0024-9297/87/2220-0819$01.50/0

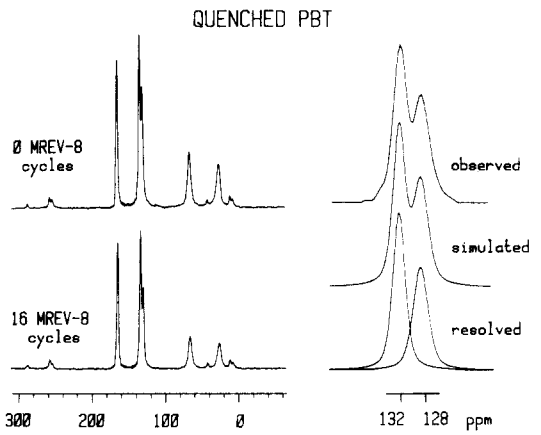

Figure 1. Dipolar rotational spin-echo 15.1-MHz ^{13}C NMR spectra of quenched poly(butylene terephthalate) at room temperature as a function of the number of semiwindowless MREV-8 cycles used during ^1H–^{13}C dipolar evolution. A 2-ms proton–carbon cross-polarization preparation of carbon magnetization preceded the dipolar evolution. The aromatic carbon region can be resolved by the deconvolution of two Lorentzians (right).

Table II
15.1-MHz ^{13}C Spin–Lattice Relaxation Times for Poly(butylene terephthalate)

	$\langle T_1(C)\rangle$,[a] ms		
thermal history	protonated aromatics[b]	$-OCH_2-$	$-CH_2-$
quenched	1120	133	98
annealed	2460	196	123

[a] Least-squares fit (95% confidence level) over the first 10% of the decay curve. [b] Resonance at 128 ppm. Overlap with 132 ppm peak not removed by computer deconvolution.

(Figure 1, bottom left). Spectra of annealed PBT have the same appearance as those of the quenched material.

Annealing lengthens the protonated aromatic carbon $\langle T_{1\rho}\rangle$ but shortens slightly the methylene carbon $\langle T_{1\rho}\rangle$'s (Table I). The interior methylene carbon $\langle T_{1\rho}\rangle$ is somewhat shorter than that of $-OCH_2-$ for both quenched and annealed PBT.[16] The $H_1(C)$ dependence of these $\langle T_{1\rho}(C)\rangle$'s is sufficiently weak that there is no doubt that relaxation is dominated by spin–lattice (motional) pathways.[12] All $T_1(C)$'s for PBT increase after annealing (Table II).

The $T_1(C)$ plots for most of the carbons of PBT have clearly visible dispersions of relaxation rates. The plot for the protonated aromatic carbon line of annealed PBT, for example, drops to less than half-value by 5 s (Figure 2, bottom), but then to only 90% relaxation by 20 s (not shown). Past t = 0.5 s, no three points of this plot are connected by a straight line. The 128 ppm protonated aromatic carbon line of quenched PBT has a particularly pronounced $T_1(C)$ dispersion, with about a 10% contribution from a fast-relaxing component (Figure 2, top). This component is completely removed by annealing. There are no abrupt changes in the curvatures of the methylene carbon T_1 plots for both quenched and annealed PBT.

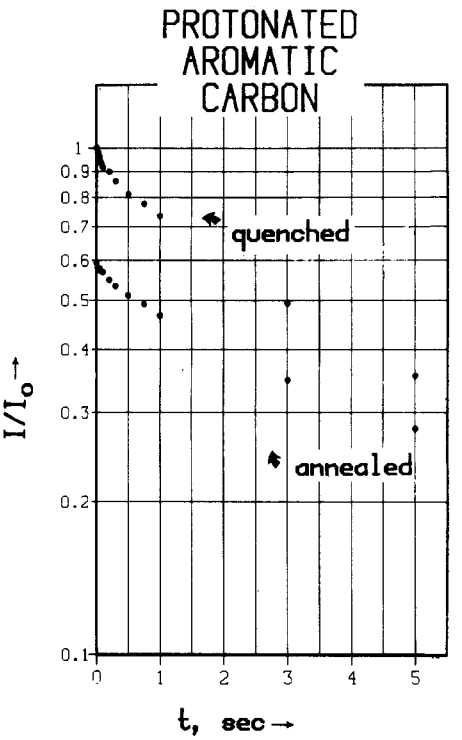

Figure 2. 15.1-MHz $T_1(C)$ plots for the protonated aromatic carbon line (128 ppm) of quenched (top) and annealed (bottom) poly(butylene terephthalate).

Dipolar Sideband Patterns. The protonated aromatic carbon dipolar line shape is influenced by the fast $T_1(C)$ component. The centerband of the pattern is exaggerated for the full sample (Figure 3, top left). When the dipolar modulation experiment is performed with a carbon preparation that includes a 200-ms $T_1(C)$ waiting period to allow the fast-relaxing component to escape, the centerband intensity is reduced (Figure 3, bottom left). The normalized difference between the two sideband patterns (Table III, row 3) is consistent with a component with

Table III
Dipolar Rotational Sideband Intensities[a] for Poly(butylene terephthalate)

thermal history	carbon	sideband no. 0	1	2	3	4	5	6
quenched	protonated aromatic[b]	0.155	0.128	0.160	0.079	0.037	0.013	0.005
	protonated aromatic, less fastest 10% $T_1(C)$ component[b,c]	0.114	0.123	0.165	0.086	0.044	0.019	0.005
	difference, normalized	0.348	0.132	0.096	0.035	0.009	0.000	0.025
	$-OCH_2-$	0.164	0.128	0.100	0.086	0.064	0.032	0.009
	$-CH_2-$	0.165	0.131	0.102	0.086	0.061	0.030	0.008
annealed	protonated aromatic[b]	0.124	0.129	0.166	0.083	0.039	0.015	0.004
	protonated aromatic, less fastest 10% $T_1(C)$ component[b,c]	0.121	0.122	0.164	0.084	0.044	0.016	0.006
	$-OCH_2-$	0.153	0.127	0.102	0.086	0.063	0.035	0.011
	$-CH_2-$	0.179	0.143	0.110	0.082	0.048	0.023	0.006
	methylene, less fastest 50% $T_1(C)$ component[e]							
	$-OCH_2-$	0.139	0.123	0.094	0.083	0.073	0.042	0.016
	$-CH_2-$	0.148	0.116	0.100	0.085	0.066	0.035	0.024

[a] Semiwindowless MREV-8 multipulse decoupling. Theoretical scale factor is 0.54. Magic-angle spinning at 1859 Hz. [b] Resonance at 128 ppm. Overlap with 132 ppm peak removed by computer deconvolution. [c] $T_1(C)$ delay of 200 ms. [d] $T_1(C)$ delay of 300 ms. [e] $T_1(C)$ delay of 115 ms.

Table IV
Experimental and Calculated Dipolar Rotational Sideband Intensities[a] for Two Crystalline Model Compounds

expt or calcn	carbon	sideband no. 0	1	2	3	4	5	6
dimethoxybenzene, expt	CH	0.115	0.123	0.168	0.086	0.043	0.016	0.007
static, calcn[b,c]	CH	0.124	0.133	0.185	0.070	0.034	0.012	0.004
[2-^{13}C]glycine, expt	CH_2	0.161	0.129	0.090	0.071	0.066	0.044	0.020
static, calcn[b,d]	CH_2	0.139	0.116	0.086	0.080	0.069	0.043	0.023

[a] Semiwindowless MREV-8 multiple-pulse decoupling. Theoretical scale factor is 0.54. Magic-angle spinning at 1859 Hz. [b] Effective scale factor is 0.39. [c] Details of the calculation are described in ref 7. [d] The CH_2 pattern is the sum of patterns calculated for proton spins parallel and antiparallel, respectively. The CH bond length is 1.09 Å, and the HCH bond angle is 109°.

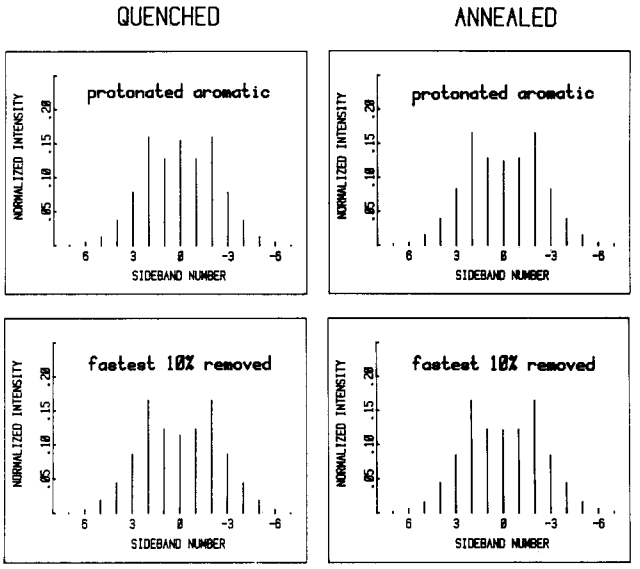

Figure 3. Experimental dipolar sideband patterns for the aromatic CH pairs of quenched (left) and annealed (right) poly(butylene terephthalate) under magic-angle spinning at 1859 Hz. The two patterns at the bottom of the figure involved a 200-ms (left) or 300-ms (right) T_1(C) delay in the preparation step of the dipolar modulation experiment to allow the 10% fastest relaxing carbons in each sample to escape.

several types of large-amplitude motions.[7] The protonated aromatic carbon resonance of annealed PBT shows no behavior of this sort (Figure 3, top and bottom right, and Table III, rows 6 and 7). These patterns are almost those expected for a static CH pair (Table IV, rows 1 and 2).

The two methylene carbon dipolar patterns of quenched PBT are indistinguishable (Table III, rows 4 and 5), while those of the annealed material are different (Figure 4, right). For annealed PBT, the $-CH_2-$ dipolar pattern has more intensity in the center and less in the wings than the $-OCH_2-$ pattern (Table III, rows 8 and 9). The difference between dipolar patterns is reduced for the methylene carbons of annealed PBT with long T_1(C)'s (Table III, rows 10 and 11). The latter patterns are both close fits to a calculated static CH_2 pattern (Table IV, row 4).

Discussion

Large-Amplitude Motion and T_1(C) Dispersions in PBT. Consistent with the earlier ^{2}D NMR studies of PBT,[1,2] the abrupt change in curvature in the plot of Figure 2 (top) demonstrates the presence in quenched PBT of a short-T_1 component. The narrow dipolar line shape of the protonated aromatic carbons of this component (Table III, row 3) is consistent with the rings undergoing 180° flips and large-amplitude oscillations and wiggles.[1,7] The wiggling is presumably part of the lattice distortions that enable ring flips.[8] The fast-relaxing component of quenched PBT (which makes up some 10% of the sample at room temperature) is removed by annealing at $T > T_g$, and so it can be reasonably associated with conformational

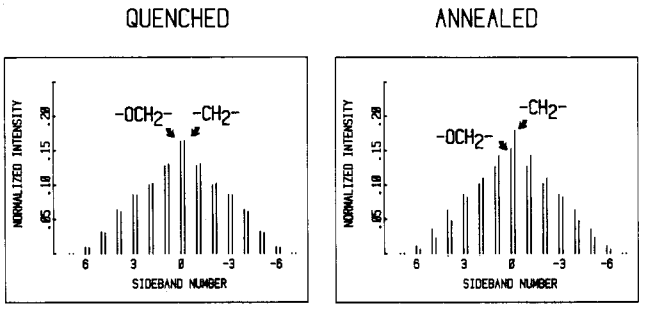

Figure 4. Experimental dipolar sideband patterns for the methylene carbons of quenched (left) and annealed (right) poly(butylene terephthalate) under magic-angle spinning at 1859 Hz.

defects in the amorphous regions of the polymer.

While the $T > T_g$ annealing has definitely removed some conformational defects, it could not have increased the crystallinity[17] of the sample by much more than 10%, as judged by the almost unchanged X-ray diffraction powder patterns (not shown). Thus, the annealed sample necessarily retains amorphous character. Using NMR to determine the concentration of the remaining conformational defects in this sample is not easy, however. The uniform curvature of the T_1(C) plot for the protonated aromatic carbon line (Figure 2, bottom) makes a quantitative assessment of the amorphous content by T_1 discrimination essentially arbitrary. Only when clear differences in relaxation behavior are apparent (as in Figure 2, top) is it possible to establish a reliable lower limit to the amorphous content.

Static Dipolar Patterns in PBT. The ring and methylene carbons of the long-T_1(C) fraction of annealed PBT have dipolar patterns (Table III, rows 7 and 10 and 11, respectively) which are close to those of crystalline model compounds (Table IV, rows 1 and 3). The widths of these patterns have been reduced by ultra-high-frequency motions common to all solids at room temperature.[18] We account for this reduction by the use of an "effective" multiple-pulse scale factor,[5] so that simulations like those of Table IV of the "static" dipolar line shapes observed for typical organic crystals then lead to the same C–H bond lengths as neutron-scattering determinations. The PBT ring carbon and methylene carbon dipolar patterns of the full sample (Table III) are reduced slightly from static patterns by the small-amplitude wiggling responsible for the fast T_1 and $T_{1\rho}$ relaxation in the amorphous regions. These motions are discussed in the next section.

Main-Chain Motions in PBT and Comparisons to Motions in Poly(ethylene terephthalate). The weak H_1(C) dependence of the methylene carbon $\langle T_{1\rho} \rangle$'s for both quenched and annealed PBT (Table I) indicates that the frequencies of cooperative main-chain motions are much greater than the 50-kHz rotating-frame Larmor frequency. The frequencies of these motions are also much greater

than those of the corresponding motions in poly(ethylene terephthalate) (PET). Thus, $T > T_g$ annealing of PBT improves packing in the amorphous regions, lowers the average frequency of megahertz-regime cooperative main-chain motions, and *lowers* the methylene carbon $\langle T_{1\rho} \rangle$. This is in contrast to the $T < T_g$ annealing of PET,[19] which lowers the frequency of main-chain motions already in the low-kilohertz regime and so *increases* the methylene carbon $\langle T_{1\rho} \rangle$. In addition, unlike the situation for PBT, protonated aromatic carbon dipolar sideband patterns[20] and ^{2}D quadrupolar line shapes[21] show that at room temperature none of the rings of quenched PET are flipping, at least at frequencies of 10^4 Hz or more. However, the average ring-oscillation frequency is still greater than 50 kHz. Thus, $T < T_g$ annealing increases spectral density at the rotating-frame Larmor frequency for the ring carbons of PET and shortens $\langle T_{1\rho}(C) \rangle$,[19] opposite to the effect of $T > T_g$ annealing on PBT in which loss of the ring-flip population dominates relaxation. Finally, annealing at $T < T_g$ has no observable effect on amplitudes of either ring or methylene carbon motions in PET as judged by unchanged dipolar sideband patterns.[20] This means the observed changes in PET relaxation rates due to $T < T_g$ annealing are primarily due to changes in the frequencies rather than amplitudes of motion. This is not the situation for the $T > T_g$ annealing of PBT, as discussed in the following section.

Asymmetry and Main-Chain Motions in PBT. The asymmetry in the main-chain motion of the shorter $T_1(C)$ component of annealed PBT is apparent in differences in the $-CH_2-$ and $-OCH_2-$ dipolar patterns (Figure 4, right, and Table III, rows 8 and 9). The interior methylene carbon pattern is the more motionally averaged of the two, consistent with the results of ^{2}D NMR experiments.[2] These differences do not appear for the quenched material (Figure 4, left). This means the constraints of tight interchain packing in, or the influence of microcrystalline domains on, the amorphous regions must be responsible for the asymmetry. In the loosely packed quenched PBT, major asymmetry in the amplitudes of methylene carbon motion is not prominent at room temperature, although minor asymmetry is present as indicated by slight differences in $\langle T_{1\rho}(C) \rangle$'s and $\langle T_1(C) \rangle$'s (Tables I and II). The results of Figure 4 emphasize that the Helfand[3,4] three-bond motion, which has been invoked to explain asymmetry in the methylene carbon motion,[2] should not be considered in terms of an isolated single chain in a vacuum, but rather in terms of a chain embedded in an interactive matrix.

Registry No. PBT (SRU), 24968-12-5; PBT (copolymer), 26062-94-2; $(H_3CO)_2C_6H_4$, 27598-81-8; [2-^{13}C]glycine, 20220-62-6.

References and Notes

(1) Cholli, A. L.; Dumais, J. J.; Engel, A. K.; Jelinski, L. W. *Macromolecules* **1984**, *17*, 2399.
(2) Jelinski, L. W.; Dumais, J. J.; Engel, A. K. *Macromolecules* **1983**, *16*, 492.
(3) Helfand, E.; Wasserman, Z. R.; Weber, T. A. *J. Chem. Phys.* **1980**, *73*, 526.
(4) Helfand, E.; Wasserman, Z. R.; Weber, T. A.; Skolnick, J.; Runnels, J. H. *J. Chem. Phys.* **1981**, *75*, 4441.
(5) Schaefer, J.; McKay, R. A.; Stejskal, E. O.; Dixon, W. T. *J. Magn. Reson.* **1983**, *52*, 123.
(6) Schaefer, J.; Sefcik, M. D.; Stejskal, E. O.; McKay, R. A.; Dixon, W. T.; Cais, R. E. *Macromolecules* **1984**, *17*, 1107.
(7) Schaefer, J.; Stejskal, E. O.; McKay, R. A.; Dixon, W. T. *Macromolecules* **1984**, *17*, 1479.
(8) Schaefer, J.; Stejskal, E. O.; Perchak, D.; Skolnick, J.; Yaris, R. *Macromolecules* **1985**, *18*, 368.
(9) Schaefer, J.; Stejskal, E. O. *Top. Carbon-13 NMR Spectrosc.* **1979**, *3*, 284.
(10) Stejskal, E. O. U.S. Patent 4 446 430, May 1, 1984.
(11) Torchia, D. A. *J. Magn. Reson.* **1978**, *30*, 613.
(12) Schaefer, J.; Sefcik, M. D.; Stejskal, E. O.; McKay, R. A. *Macromolecules* **1984**, *17*, 1118.
(13) Munowitz, M. G.; Griffin, R. G. *J. Chem. Phys.* **1982**, *76*, 2848.
(14) Burum, D. P.; Linder, M.; Ernst, R. R. *J. Magn. Reson.* **1981**, *44*, 173.
(15) Spiess, H. W. *Colloid Polym. Sci.* **1983**, *261*, 193.
(16) Jelinski, L. W.; Dumais, J. J.; Watnick, P. I.; Engel, A. K.; Sefcik, M. D. *Macromolecules* **1983**, *16*, 409.
(17) Yokouchi, M.; Sakakibara, Y.; Chatani, Y.; Tadokoro, H.; Tanaka, T.; Kentaro, Y. *Macromolecules* **1976**, *9*, 266.
(18) Greenfield, M. S.; Vold, R. L.; Vold, R. R. *J. Chem. Phys.* **1985**, *83*, 1440.
(19) Sefcik, M. D.; Schaefer, J.; Stejskal, E. O.; McKay, R. A. *Macromolecules* **1980**, *13*, 1132.
(20) Schaefer, J., unpublished data.
(21) Vega, A. J., unpublished data.

Theory of Polydispersity Effects on Polymer Rheology. Binary Distribution of Molecular Weights

Michael Rubinstein† and Eugene Helfand*

AT&T Bell Laboratories, Murray Hill, New Jersey 07974

Dale S. Pearson

Corporate Research Laboratories, Exxon Research and Engineering Company, Annandale, New Jersey 08801.

Received August 1, 1986

ABSTRACT: Effects of polydispersity on rheological properties of entangled polymers are analyzed. A number of models of tube renewal are discussed and compared with each other and with experiments. A theory incorporating reptation, tube renewal, and fluctuations in the tube length into a general description of stress relaxation is developed. Dynamical moduli were calculated for monodispersed and bidispersed systems and compared with experiments. The product of viscosity and recoverable shear compliance is predicted to be of the order of the longest relaxation time of the higher molecular weight component with a weak dependence on the relative volume fraction of the binary mixture for a large enough concentration of longer molecules.

I. Introduction

Polydispersity has a profound effect on the viscoelastic properties of polymers. This is to be expected, since the fundamental relaxation times in the system, the reptation times of the molecules, vary as a high power of molecular weight.

In this paper we explore some theoretical aspects of polydispersity, in particular its effects on the stress relaxation and dynamical moduli, and compare the theo-

† Present address: Research Laboratories, Eastman Kodak Co., Rochester, NY 14650.

0024-9297/87/2220-0822$01.50/0